frontiers | Frontiers in Earth Science

TYPE Review
PUBLISHED 23 December 2022
DOI 10.3389/feart.2022.1055255

OPEN ACCESS

EDITED BY
Martyn Tranter,
Aarhus University, Denmark

REVIEWED BY
William Prescott Leeman,
Rice University, United States
Ian Ernest Masterman Smith,
The University of Auckland,
New Zealand

*CORRESPONDENCE
Jian Wang,
wangj95@cardiff.ac.uk,
wangjian330921@163.com

SPECIALTY SECTION
This article was submitted to Geochemistry,
a section of the journal
Frontiers in Earth Science

RECEIVED 27 September 2022
ACCEPTED 13 December 2022
PUBLISHED 23 December 2022

CITATION
Wang J, Gleeson M, Smith WD, Ma L, Lei Z, Shi G and Chen L (2022), The factors controlling along-arc and across-arc variations of primitive arc magma compositions: A global perspective.
Front. Earth Sci. 10:1055255.
doi: 10.3389/feart.2022.1055255

The factors controlling along-arc and across-arc variations of primitive arc magma compositions: A global perspective

Jian Wang[1]*, Matthew Gleeson[1], William D. Smith[1,2], Lin Ma[3], Zhibin Lei[1], Guanghai Shi[4] and Long Chen[5]

[1]School of Earth and Environmental Sciences, Cardiff University, Cardiff, United Kingdom, [2]Department of Earth Sciences, Carleton University, Ottawa, ON, Canada, [3]State Key Laboratory of Isotope Geochemistry, Guangzhou Institute of Geochemistry, Chinese Academy of Sciences, Guangzhou, China, [4]State Key Laboratory of Geological Processes and Mineral Resources, China University of Geosciences, Beijing, China, [5]Key Lab of Submarine Geosciences and Prospecting Techniques, Ocean University of China, Qingdao, China

Arc volcanism is a key process influencing Earth's climate, continental growth, and the formation of mineral deposits. Therefore in this contribution, we have compiled whole-rock geochemistry of frontal arc and rear-/back-arc basalts, crustal thickness, and slab parameters (e.g., slab age, slab dip, and convergence velocity) from global convergent margins to investigate the factors controlling along-arc and across-arc variations. Crustal thickness or lithosphere thickness plays a dominant role in elements immobile in aqueous fluids (e.g., Zr/Yb and Nb/Yb). The effect is imposed through mantle partial melting for both frontal arc and rear-/back-arc rocks. Slab thermal structure also affects these immobile elements and gives rise to along-arc variations. Both slab sediment and altered oceanic crust can melt especially in hot subduction zones which yield across-arc variations (e.g., Nd isotope). Aqueous fluids (represented by element ratios such as Ba/Nb and Sr/Nd) also show across-arc variations as they decrease toward rear-/back-arc. This meanwhile decreases mantle wedge melting as rear-/back-arcs show higher Zr/Yb and Nb/Yb. However, no correlations between aqueous fluids and slab parameters suggest aqueous fluids in arc rocks are controlled by complex processes. We summarize factors such as slab alteration, slab dehydration, and mantle metasomatism might impose an effect on the content of fluid mobile elements in arc rocks.

KEYWORDS

primitive arc magma, crustal thickness, slab thermal structure, frontal arc, rear-arc, back-arc, along-arc variations, across-arc variations

1 Introduction

Arc magmatism is a critical process in the formation of continental crust (e.g., Plank, 2005; Lee et al., 2007; Lee et al., 2012; Kelemen, 2013), climate change (e.g., CO_2 recycling; Johnston et al., 2011), and the formation of economically important mineral deposits (e.g., Cu-porphyry and Li deposits; Chiaradia, 2015; Chen et al., 2020; Barber et al., 2021). Magmatism in arc settings is fundamentally related to the dehydration (Pearce and Peate, 1995; Schmidt and Poli, 1998; Tatsumi, 2005; Grove et al., 2009) and melting (Defant and Drummond, 1990; Skora and Blundy, 2010) of subducting lithospheric components at high pressures and temperatures. The liberated fluids (including aqueous fluids and melts) ascend into the overlying mantle wedge, where they substantially lower the solidus temperature of the mantle wedge, thus driving hydrous mantle melting (up to 2 wt.% H_2O in bulk peridotite; Grove et al., 2009; Grove et al., 2012) and ultimately volcanic activity (Davies and Stevenson, 1992; Grove et al., 2009; Grove et al., 2012; Schmidt and Poli, 2014; Zheng et al., 2020). Therefore, arc magmatism differs from that in plume-related or mid-ocean ridge systems, where magma forms through only adiabatic decompression melting (Klein and Langmuir, 1987; Langmuir et al., 1992; Niu, 1997) of relatively water-poor mantle reservoirs (<.02 wt.% H_2O; Asimow and Langmuir, 2003; Green et al., 2010).

A global correlation between overriding arc crustal thickness and arc basalt composition has been addressed by several studies (Plank and Langmuir, 1988; Mantle and Collins, 2008; Turner and Langmuir, 2015; Niu, 2021). This correlation can be attributed to crustal or lithosphere thickness modulating degrees of mantle melting (Plank and Langmuir, 1988; Niu, 2021) based on the hypothesis that arc magmas derive from flux-assisted decompression melting (Plank and Langmuir, 1988; Niu, 2021). Another interpretation suggests thickened lithosphere cools down the mantle wedge by depressing its isotherm which reduces degrees of mantle melting (Turner and Langmuir, 2015). Given the processes involved in the genesis of arc magmas, it is common that the composition of arc primary melts displays a clear influence of slab fluids (generating the so-called "arc signature," i.e., Nb-Ta trough due to the enrichment of Ba, Th, U, and La on the multi-element diagram) (Pearce and Peate, 1995; Tatsumi, 2005). Despite the importance of aqueous fluids on primitive magma composition and mantle melting, the processes of mantle wedge beneath arc fronts being hydrated by these fluids are not well understood. The release of aqueous fluids is suggested to be significant for the uppermost part of the slab beneath and above the sub-arc depth (van Keken et al., 2011; Schmidt and Poli, 2014). The aqueous fluids that metasomatize the mantle source of arc magmas derive from dehydration of hydrous minerals in the subducting slab (Grove et al., 2009) or fore-arc mantle wedge (Tatsumi et al., 1986; Davies and Stevenson, 1992; Hattori and Guillot, 2003; Tonarini et al., 2011).

In this study, we have compiled arc basalt geochemistry and parameters of the subducting plate (e.g., slab dip, convergence velocity, and slab age) and the overriding plate (e.g., crustal thickness) from convergent margins to investigate the relative roles of slab materials and crustal thickness on the along- and across-arc variations.

2 Data compilation

Subduction zones can be divided into frontal arc and rear-arc or back-arc magmatic systems (Figure 1). Both rear-arc and back-arc volcanic systems are typically located behind the frontal arc (Taylor and Nesbitt, 1998), and we differentiate between the two based on the presence (back-arc; e.g., the East Scotia Ridge and Central Mariana Trough) or absence (rear-arc; e.g., the Reventador-Sumaco-Puyo rear-arc in the northern Andes and Apoyo rear-arc in Central America) (Duggen et al., 2007; Ancellin et al., 2017) of active spreading. In this study, a rear-arc system is considered to lie >30 km behind the Holocene volcanic front, where the location is based on data from the Smithsonian Global Volcanism Program (Global Volcanism Program, 2013). While arc magmatism is commonly associated with the dehydration and melting from a subducting slab (Tatsumi et al., 1986; Defant and Drummond, 1990; Pearce and Peate, 1995; Schmidt and Poli, 1998; Skora and Blundy, 2010), it can also occur in regions above a "slab window" (that is, an asthenosphere-filled gap that forms between a pair of diverging, subducting oceanic plates in response to ridge subduction; Thorkelson and Breitsprecher, 2005). These slab windows allow hotter asthenospheric mantle from below the subducted plate to ascend into the mantle wedge and melt. Examples of arc magmatism associated with slab windows include Tahoe-Truckee in the Cascades arc (Juan de Fuca-Pacific plate boundary; Cousens et al., 2011), Costa Rica/Western Panama (Cocos-Nazca plate boundary; Abratis et al., 2001), Taitao and Hudson in the South Andes (Nazca-Antarctic plate boundary; Gutiérrez et al., 2005), and Solomon arc (Solomon Sea plate spreading centre; Schuth et al., 2009). We exclude these locations from our compilation as magmatism associated with slab windows is primarily driven by asthenospheric decompression melting (Thorkelson, 1996) and slab margin melting (Thorkelson and Breitsprecher, 2005), which is different from arc magmatism. Similarly, arc systems with continental rifting such as the Trans-Mexican Volcanic Belt (Verma et al., 2016), where flux melting might play a minor role if any, in arc magmatism are also not considered. Cases of mantle wedge affected by mantle plume such as in North Tonga (i.e., Beier et al., 2017; Wendt et al., 1997) are also excluded. In addition, we only include samples that were collected from regions of oceanic plate subduction, i.e., we excluded any

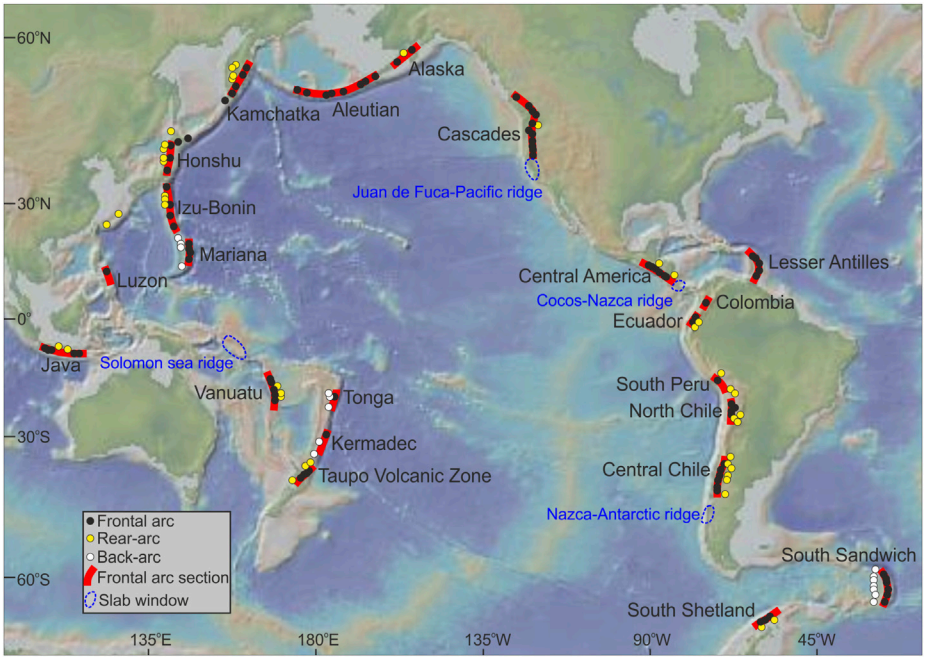

FIGURE 1
Quaternary arc volcanos compiled for this study. The background map was processed with GeoMapApp (https://www.geomapapp.org).

rocks that were sampled from regions of continental plate subduction beneath an oceanic plate (Batu Tara in Bunda arc) or continental plate (Aeolian arc, Aegean arc, Apenninic arc). Bismarck arc in a complex setting with several active subduction zones nearby (Ryan and Marlow, 1988; Woodhead et al., 1998; Bird, 2003; Tregoning and Gorbatov, 2004) is also not discussed here.

2.1 Geochemical data

We compiled Quaternary volcanic rocks from continental and oceanic arcs from GEOROC in December 2019 (Appendix A). These data represent the recent volcanic history of continental and oceanic arcs worldwide and, therefore, mitigate temporal changes in magma chemistry. A series of filters are applied to our geochemical data to ensure the compiled samples reflect primitive magmas.

Firstly, rocks with a sum of major elements between 97 and 101.5 wt% (Farner and Lee, 2017; Schmidt and Jagoutz, 2017) were considered to minimise the effects of chemical alteration. Data with Nb/Ta>30 were removed due to the possibility of analytical error (Elliott, 2003; Pearce et al., 2005; Beier et al., 2017). Secondly, we only consider samples with 6–16 wt% MgO which are mainly basalt with a few andesites to ensure that our samples are minimally affected by fractional crystallisation or crustal assimilation. The lower limit of MgO (6 wt%) was selected as crustal assimilation and fractionation of minerals other than olivine tend to be most apparent below this value (Turner et al., 2016) and the upper limit (16 wt%) is based on the equilibrium between primitive melts and mantle olivine (Schmidt and Jagoutz, 2017). More than 90% have Eu_N/Eu^* between .9–1.2 which suggests the effect of plagioclase crystallization is minor (Appendix B1). As a result, trace element ratios such as Zr/Yb, Nb/Yb, Sr/Nd, Ba/Nb, Ba/La, and Th/Nb (each data point has analysed values for these elements) and isotopes in our filtered data likely reflect the primitive melt composition. After filtering, the data were averaged within volcanoes and then the averaged volcanos were averaged for arc sections (based on the definition by Syracuse and Abers, 2006). The compiled database contained major element, trace element, and Nd isotope data from 228 volcanos (150 frontal arc volcanos and 78 rear-/back arc volcanos) split across 60 arc sections (34 frontal arc sections and 26 rear-/back-arc sections).

2.2 Crustal thickness

Crustal thickness estimates are highly dependent on seismic data quality and the crustal velocity structure (Zellmer, 2008). To minimise uncertainty caused by variable data quality in different arc segments, we obtain crustal thickness estimates from CRUST 1.0 (Laske et al., 2013). The Moho depth in CRUST1.0 is based on 1-degree averages crustal thickness from active source seismic

studies as well as from receiver function studies. For cells with no such constraints, crustal thicknesses are estimated using gravity constraints. For cells with no local seismic or gravity constraints, statistical averages of crustal thickness were extrapolated (Laske et al., 2013). Each 1 × 1-degree cell in CRUST 1.0 has a unique 8-layers profile which includes water, ice, upper sediments, middle sediments, lower sediments, upper crust, middle crust, and lower crust. One-third of arc volcanos in this study are underwater and most of the water depths are <2 km. The crustal thickness in this study is the sum of the sediment layer and crust layer. The averaging method for arc sections is the same as that for geochemical data above, which is also the same as slab parameters below.

2.3 Slab parameters

Plate boundaries were digitized and outlined by Bird (2003). The outlined plate boundaries are comprised of the "digitization step" which is the short great-circle arc between adjacent digitized plate boundary points. There are 5,819 steps (Bird, 2003) ranging from 1 to 109 km with a mean length of 44.7 km. Each step has an estimate of the divergent component of relative velocity convergence, which is considered as the convergence velocity in the present study. Another important parameter for this study is the age of the slab crust below the volcanic arcs. These ages are represented by the age of the slab at the plate boundary and can be estimated using the age grid of Müller et al. (2008). The latitude and longitude of age sites are the same or close to the ones chosen for the convergence velocity. Slab dip and slab sub-arc depth for each volcano is from Hayes et al. (2018). If no data is available for a particular location, the values from the closest volcano to that location are chosen.

3 Results and discussion

Beneath each volcanic arc, different volumes of slab-derived aqueous fluids, sediment melts, and altered oceanic crust (AOC) melts metasomatize the overlying ambient mantle wedge which enrichs the mantle in fluid-mobile elements such as large ion lithophile elements (LILEs), light rare earth elements (LREEs), and Th relative to N-MORB (Pearce and Peate, 1995; Pearce et al., 2005; Zheng, 2019) and may also modify the mantle isotopic signature (e.g., Sr, Nd, Pb, B; Leeman et al., 1994; Elliott, 2003; Cooper et al., 2020). As aqueous fluids increase the content of LILEs through mass transfer but also decrease it through increasing the degree of mantle melting, it is inappropriate to use the concentration or ratios of LILEs to investigate the melt fraction of the mantle wedge. Instead, it is necessary to consider the ratios of fluid-immobile elements that are fractionated during mantle melting (e.g., Zr/Yb, Nb/Yb) to evaluate the degree of mantle melting and ratios of fluid-mobile to fluid-immobile trace elements that are not fractionated during mantle melting (e.g., Sr/Nd, Ba/Nb, Ba/La, Pb/Ce; Tatsumi et al., 1986; Hawkesworth et al., 1993; Brenan et al., 1995; Elliott et al., 1997; Elliott, 2003; Kessel et al., 2005; Plank, 2013) to constrain the slab aqueous fluids beneath an volcanic arc system. The ratio of fluid-immobile element Th to Nb can be considered to constrain slab sediment component which is most likely transferred as melts (Elliott et al., 1997).

Previous studies have shown that sediment has an important influence on concentrations of Ba, Sr and Th (Plank and Langmuir, 1993). However, trace element ratios, especially Ba/Nb, Sr/Nd, and Th/Nb are not correlated with sediment Ba, Sr, and Th respectively and neither with sediment thickness (Appendix B2). This finding is consistent with Patino et al. (2000) which suggests Ba, Sr, and U are less efficiently liberated from the slab to volcanos relative to other elements such as Cs, Rb, and K. This indicates indices of slab component in this study are not dictated by composition and amount of subducted sediment. Therefore, we can use these ratios to discuss other factors such as slab parameters which possibly control aqueous fluids.

3.1 The effect of crustal thickness on fluid immobile elements through mantle melting

Positive correlations between crustal thickness and incompatible element ratios of frontal arc rocks such as Zr/Y and Dy/Yb which are immobile in aqueous fluids have been addressed by several studies (Mantle and Collins, 2008; Turner and Langmuir, 2015; Turner et al., 2016). Our data reveals that Zr/Yb and Nb/Yb show positive correlations with crustal thickness, in agreement with Turner and Langmuir (2015) (Figures 2A,B). Besides, after ruling out the effect of the slab thermal parameter (discussed below), the partial correlation coefficient for crustal thickness *versus* Zr/Yb is .705 with a 2-tailed significance smaller than .001 and the partial correlation coefficient for crustal thickness *versus* Nb/Yb is .560 with the significance smaller than .001. This suggests a significant linear correlation between crustal thickness and Zr/Yb or Nb/Yb and therefore crustal thickness plays an important role on ratios of incompatible elements such as Zr/Yb and Nb/Yb.

In addition, these correlations also occur in rear-arc/back-arc rocks (Figure 2). The R-square (i.e., .683) is greater than the frontal arc rocks in crustal thickness *versus* Zr/Yb. The partial correlation coefficient is also high in both diagrams. All of these indicate crustal thickness plays an important role in controlling the primitive magma composition for both frontal arc and rear-/back-arc systems. In other words, crustal thickness controls along-arc variations for both systems. The plots for arcs above slab window are sparse which suggests different and complex processes of mantle melting in this tectonic setting.

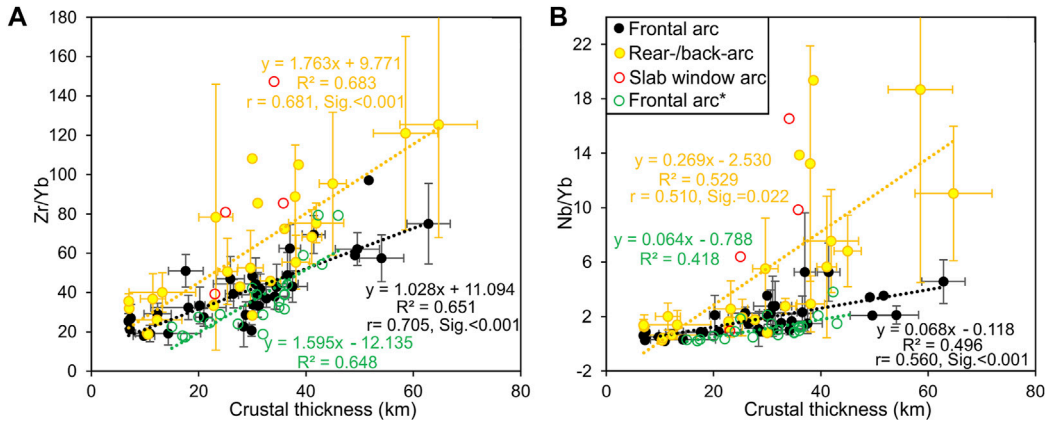

FIGURE 2
Crustal thickness of the overriding plate vs. immobile incompatible trace element ratio Zr/Yb **(A)** and Nb/Yb **(B)**. The partial correlation coefficient r is calculated when the slab thermal parameter (discussed below) is taken as the control variable, with 2-tailed significance. The rear-arc in Java (Muriah and Ringgit-Besar volcano) which has extremely high Nb/Yb is excluded in B and other figures below. Frontal arc* from Turner and Langmuir (2015) is also plotted for comparison. As these two ratios are not given in their paper so they are calculated based on the average trace element ratios given in their supplement. For example, Zr/Yb = average La/Yb divided by average La/Zr.

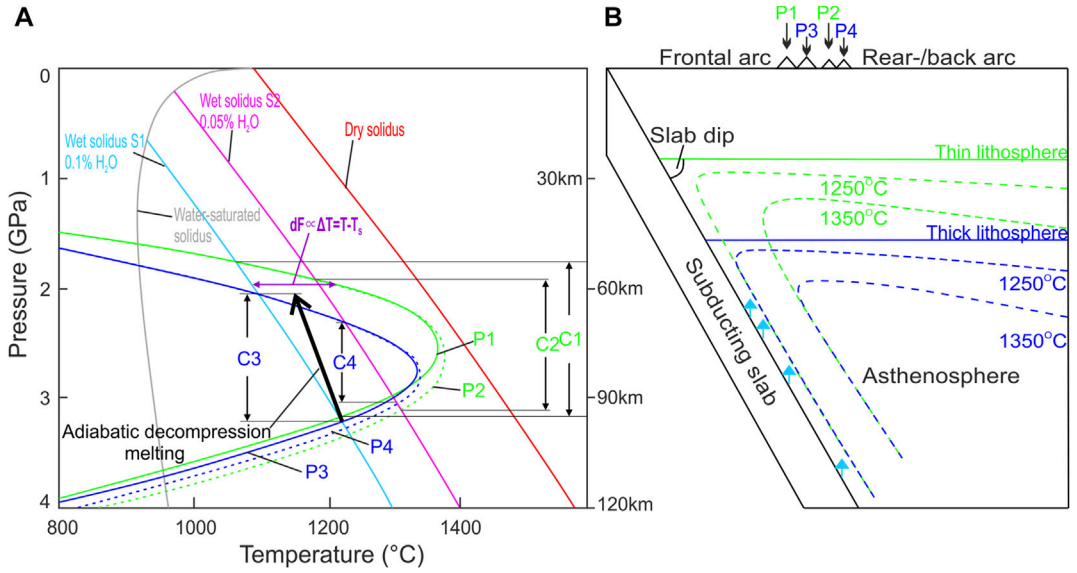

FIGURE 3
(A) A phase diagram to illustrate how crust or lithosphere thickness and slab-derived aqueous fluids exert their effects on across- and along-arc variations through mantle melting degrees [solidus is from Katz et al., 2003: wet solidus S1 is the solidus with .1% water and wet solidus S2 is .05% water; geotherm P1 is modified from Hall, (2012)] **(B)** A sketch to show mantle thermal structure under thin and thick crust [modified from Turner and Langmuir (2015)]. 1) Flux melting. For along-arc variation caused by lithosphere thickness, the geotherm for the mantle wedge beneath thick lithosphere is more depressed than the one beneath thin lithosphere (e.g., P3 *versus* P1). Assuming the same wet solidus S1 for both cases, the average melting degrees for the whole melting column (the area between the wet solidus and wedge geotherm divided by the vertical length C between the two intersection points) beneath thick lithosphere is lower for the one beneath thin lithosphere (area [S1-P3]/C3 vs. area [S1-P1]/C1). For across-arc variations caused by aqueous fluids, the wet solidus for the rear-arc (solidus S2) is closer to the dry solidus than the solidus for the frontal arc magmatism (solidus S1). The average mantle melting degree for the rear-arc (area [S2-P2]/C2) is smaller than the one for the frontal arc. 2) Decompression melting. When explained by decompression melting, the melting degree is represented by the length of the melting column. For example, C1 > C2 indicates the melting degree of frontal arc mantle is higher than that of the rear-/back-arc mantle and C1 > C3 indicates the melting degree of the frontal arc mantle beneath thin lithosphere is higher than that beneath thick lithosphere.

The exact processes of mantle wedge melting and melt extraction are not well understood (Plank and Langmuir, 1988; Katz et al., 2003; Grove et al., 2012; Niu, 2021). Currently, there are two main mechanisms for the crust/lithosphere thickness controlling melting degrees of mantle wedge: flux melting and decompression melting. For flux melting, a constant water content distributed evenly over a melting column is applied for simplicity (Katz et al., 2003), although the reality is more complex (Davies, 1999; Gaetani and Grove, 2004; Grove et al., 2006). Similar to adiabatic decompression melting in middle ocean ridges (Klein and Langmuir, 1987; Langmuir et al., 1992), the degree of mantle melting above the subduction zone should be the average value of melting degrees through the whole melting column. Therefore, the average melting degree can be represented by the area between the wet solidus and wedge geotherm divided by the vertical length between the two intersection points (Figure 3A). For along-arc variations in frontal arcs, the mantle wedge beneath thick lithosphere has a depressed geotherm P3 compared with P1 of the mantle wedge beneath thin lithosphere (Figures 3A,B). Assuming the mantle wedge is metasomatized by a similar volume of water, i.e., the wet solidus (e.g., S1) is the same for both cases, the average melting degree for the mantle beneath thin lithosphere is higher than the one for the mantle beneath thick lithosphere (Figure 3A). This is similar to the rear-/back-arc systems. The rear-arc beneath thick lithosphere possesses a depressed geotherm P4 compared with the P2 beneath thin lithosphere (Figure 3A). Assuming the same wet solidus S2 for both cases, the average melting degree for the mantle beneath thin lithosphere is higher than for the mantle beneath thick lithosphere. In this regard, the mantle wedge structure differs due to the overriding lithosphere thickness and the geotherm of the mantle wedge beneath thick lithosphere is depressed deeper giving rise to the lower maximum melting degree and average melting degree. Therefore, mantle thermal structure which is modulated by overriding plate thickness is the key factor controlling mantle wedge melting. For decompression melting, slab-derived fluids trigger mantle wedge melting and the hydrous melt facilitates the formation of a diapir (Niu, 2021). This diapir upwells and goes through decompression melting which stops at the base of the lithosphere where it reaches the maximum melting degree. The average melting degree of this melting column is proportional to the maximum degree similar to the case in the middle ocean ridge (Klein and Langmuir, 1987; Niu, 1997). Therefore, the longer the melting column is (C in Figure 3A), the higher the average melting degree is. The melting column under thin lithosphere (C1) is longer than that under thick lithosphere (C2) which can explain why the mantle wedge under thin lithosphere goes through the lower degree of partial melting. However, this model cannot be used to explain why the rear-/back-arc mantle has a lower melting degree than the frontal arc mantle as both systems can possess the same crust/lithosphere thickness (discussed below) unless different wet solidi are applied (Niu, 2021). In addition, the temperature of the upwelling diapir decreases and reaches a minimum at the top of the melting column during adiabatic decompression melting. Therefore, the diapir at the onset of flux melting should have a reasonably high initial temperature (not likely a water-saturated solidus temperature) as the primitive magma is ca. 1,200°C at the crust-mantle boundary (Gaetani and Grove, 2004) and the melting temperature for the mantle above cold subduction zones such as Izu-Bonin is still >1,100°C (Lee et al., 2009).

3.2 The effect of slab thermal structure on fluid immobile elements through mass transfer

Slab thermal parameter Φ/100 [Φ is the product of convergence velocity V, slab age A, and the sin value of slab dip sin?; (Kirby et al., 1991)] is used to constrain slab thermal structure. The trace element ratios correlate negatively with Φ/100 (Figure 4), consistent with previous work (Turner and Langmuir, 2015). All these correlations can also be found in rear-/back-arc rocks (Figure 4). However, as crust thickness plays a dominant role in Zr/Yb and Nb/Yb (Figure 2) and crust thickness correlates negatively with slab dip (Perrin et al., 2018) (Appendix B3), the correlation between Φ and Zr/Yb or Nb/Yb might be affected by crustal thickness. To rule out the effect of crustal thickness, partial correlation coefficient is calculated with crustal thickness as the control variable. Low significance (<.05) and intermediate |r| for frontal arcs in Figure 4A indicate slab thermal structure (represented by Φ/100) imposes an effect on immobile trace element ratios such as Zr/Yb. This suggests that these elements which are immobile in aqueous fluids can be affected by the thermal state of the subducting slab which controls mass transfer from slab to mantle wedge. However, high significances and low partial correlation coefficients for rear-/back-arcs (Figures 4A,B) indicate no significant correlation between these trace element ratios and Φ as rear-/back-arcs are further away from trench than frontal arcs. To determine how components in Φ control Zr/Yb and Nb/Yb, V, A, and sinθ *versus* Zr/Yb and Nb/Yb are plotted (Figure 5). For frontal arc rocks, all components have variable degrees of negative correlations with Zr/Yb or Nb/Yb with slab age having the highest correlation coefficients with the element ratios (Figures 5A,B).

The effect of mass transfer from the slab can also be investigated by isotope data from the frontal arc and rear-/back-arc systems. The value of ε_{Nd} [the present-day $^{143}Nd/^{144}Nd$ value .512638 of CHUR is from Goldstein et al. (1984)] is low in the subducting sediment (−13.1–2.5; Plank, 2013) but is high in the underlying MORB-like AOC (8.9–10.4 for the Pacific domain; Peate et al., 1997; Hauff et al., 2003; Werner et al., 2003; White and Klein, 2013; Shu et al., 2017). The Th/Nb value is high in slab sediment (Plank, 2013) and hence can be considered as an index for sediment input (.2–1.1; Kelemen, 2013; Turner and Langmuir, 2015). Therefore, the difference

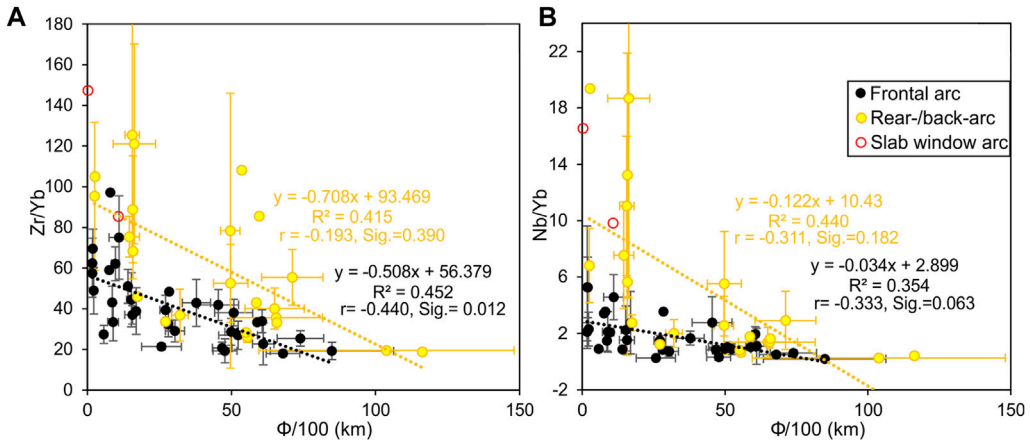

FIGURE 4
Bivariant diagrams of slab thermal parameter Φ/100 (Φ=convergence velocity × slab age × the sine of slab dip) vs. incompatible trace element ratio Zr/Yb **(A)** and Nb/Yb **(B)** of frontal arc and rear-/back-arc rocks. The partial correlation coefficient r is calculated when the crustal thickness is taken as the control variable, with 2-tailed significance.

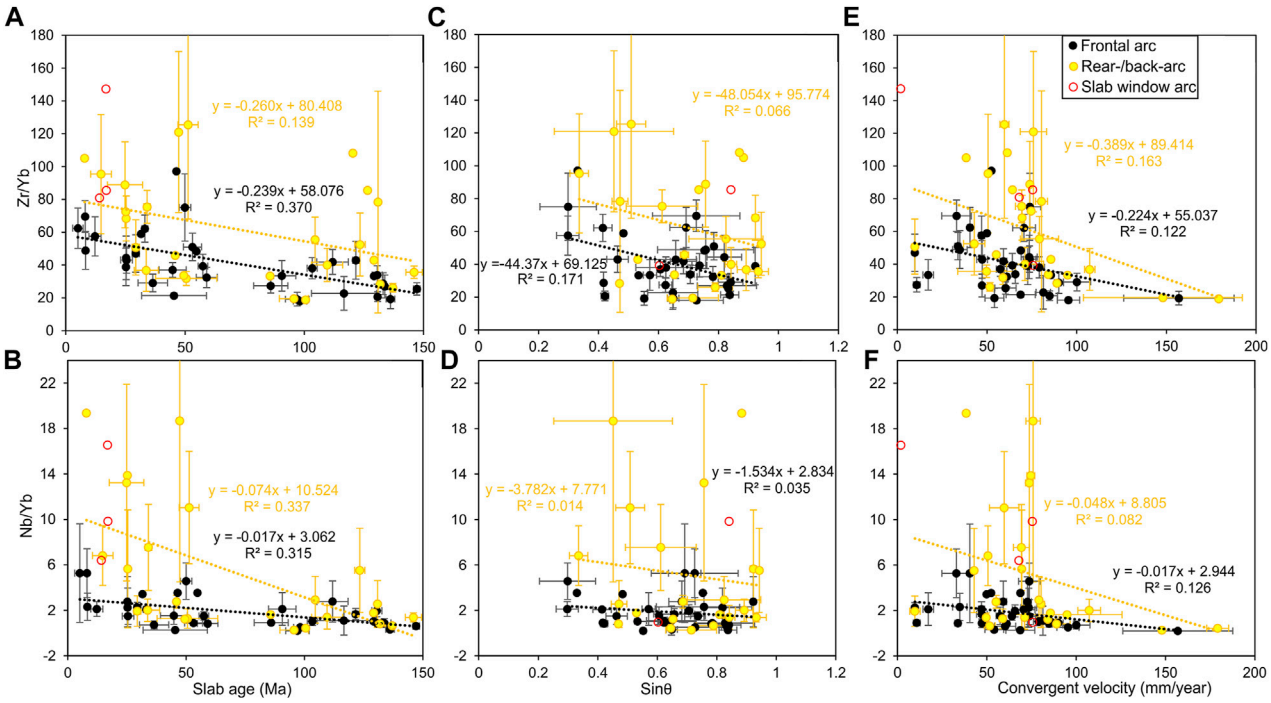

FIGURE 5
Slab parameters vs. ratios of trace elements which are immobile in aqueous fluids. Slab age vs Zr/Yb **(A)** and Nb/Yb **(B)**. Sinθ vs Zr/Yb **(C)** and Nb/Yb **(D)**. Convergent velocity vs Zr/Yb **(E)** and Nb/Yb **(F)**.

between the frontal arc and rear-/back-arc in $^{143}Nd/^{144}Nd$ and Th/Nb can provide insights into the nature and volume of slab-derived material. A negative $1000\Delta^{143}Nd/^{144}Nd$ (the value of frontal arc minus that of rear-/back-arc) is usually accompanied by a positive ΔTh/Nb. This suggests a greater sediment component in the frontal arc relative to the rear-/back-arc (Figure 6A). However, a positive $1000\Delta^{143}Nd/^{144}Nd$ can occur with a positive ΔTh/Nb in some arc sections which may be explained by a higher volume of AOC component (e.g., AOC melts) in the frontal arc. Furthermore, all arcs with positive $1000\Delta^{143}Nd/^{144}Nd$ are found in the hot subduction

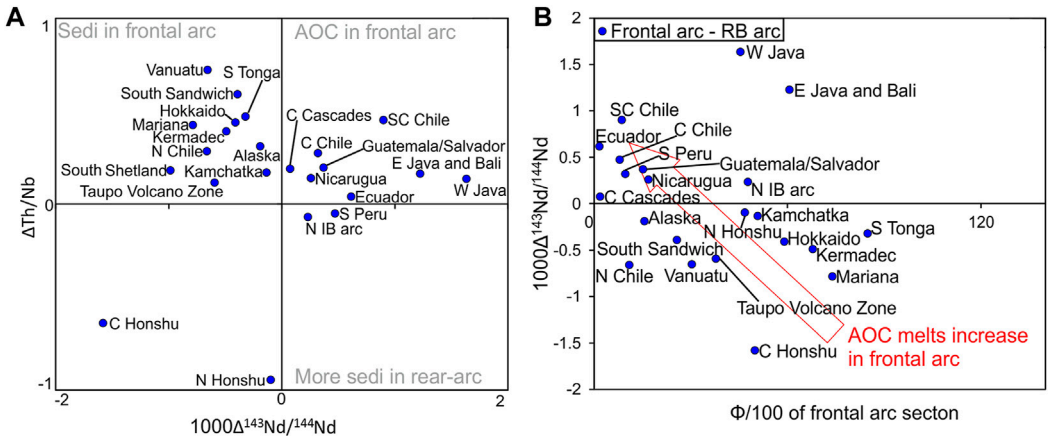

FIGURE 6
Comparison of $^{143}Nd/^{144}Nd$ and Th/Nb between the frontal arc and rear-/back-arc sections. **(A)** $1000\Delta^{143}Nd/^{144}Nd$ vs. ΔTh/Nb. Negative $1000\Delta^{143}Nd/^{144}Nd$ (frontal arc minus rear-/back-arc) with positive ΔTh/Nb indicates more sediment melts in the frontal arc than the rear-/back-arc while positive $\Delta\varepsilon_{Nd}$ with positive ΔTh/Nb indicates more AOC melts in the frontal arc. **(B)** Φ/100 vs. $1000\Delta^{143}Nd/^{144}Nd$. Positive $1000\Delta^{143}Nd/^{144}Nd$ are found in subduction zones with small Φ/100 indicating AOC can melt in hot subduction zones. The high-potassium rocks in the Java rear-arc are considered to form by partial melting of an enriched mantle (Edwards et al., 1991; Edwards et al., 1994) which shows an anomaly in B.

zone with $\Phi/100 < 20$ (Figure 6B). This is consistent with the previous idea that AOC melting can occur in a hot subduction zone (Defant and Drummond, 1990).

We conclude that slab input plays an important role in along-arc variations at frontal arcs and across-arc variations. As the subduction zone becomes hotter along arcs, more sediment melts and AOC melts can be liberated, implying that Zr and Nb may be readily mobilised in slab-derived materials [the partition coefficient between melt and solid can be >1; (Kessel et al., 2005; Hermann and Rubatto, 2009; Skora and Blundy, 2010)], and consequently, become enriched in the overlying mantle. Furthermore, sediment melts and AOC melts play an important role in across-arc chemical and isotopic variations. The amount of sediment component is higher in frontal arcs than that in rear-/back-arcs which gives rise to higher sediment-related element ratios such as Th/Nb in frontal arc magmas. Meanwhile, frontal arc magmas possess lower $1000\Delta^{143}Nd/^{144}Nd$ due to the low $^{143}Nd/^{144}Nd$ of sediment components in cold subduction zone systems. However, in hot subduction zones, AOC melts could form and more AOC melts in frontal arc magmas increases $1000\Delta^{143}Nd/^{144}Nd$ which gives rise to an across-arc variation.

3.3 Possible factors controlling the content of fluid mobile elements

The rear-/back-arcs are lower in Ba/Nb, Sr/Nd, and U/Nb (Figures 7A,B,C) in comparison to frontal arc sections with similar crustal thickness. This suggests rear-/back-arcs are less affected by slab aqueous fluids with no effect imposed by crustal thickness, which is consistent with large quantities of previous studies (Ishikawa and Nakamura, 1994; Ryan et al., 1995; Patino et al., 2000; Tollstrup et al., 2010; Leeman et al., 2017). Furthermore, rear-/back-arc systems generally have higher Zr/Yb and Nb/Yb values (Figure 2). This across-arc variation is not likely caused by mantle thermal structure as high mantle temperature can persist for a long distance from the arc to rear-/back-arc (~500 km for the Cascadia subduction zone; Currie et al., 2004; Curie and Hyndman, 2006) and both frontal arc and rear-/back-arc possess similar mantle thermal structure. Alternatively, lower mantle melting degrees by less aqueous fluids or greater input of slab melts in rear-/back-arcs are two possibilities. However, aqueous fluids should account for this across-arc variation as the rear-/back-arc is affected by less aqueous fluids (lower Ba/Nb, Sr/Nd, and U/Nb; Figures 7A,B,C) and fewer slab melts (lower Th/Nb, Figure 7D and Figure 6A) than the frontal arc. Lower volumes of slab-derived aqueous fluids metasomatizing the mantle source beneath rear-/back-arc result in lower degrees of mantle melting, consequently giving rise to higher Zr/Yb and Nb/Yb. However, mantle fertility cannot be ruled out as the mantle beneath back-arc could be more enriched or less depleted than the mantle beneath frontal arc as the melt-extracted mantle in back-arc could serve as the mantle wedge through advecting (Pearce and Parkinson, 1993; Woodhead et al., 1993). For across-arc variations, the mantle wedge under the rear-arc has a similar or slightly higher maximum temperature (geotherm P2 in Figure 3A) than the one under the frontal arc (geotherm P1). However, the efficiency of mantle metasomatism by aqueous fluids in the rear-/back-arc is low so that the wet solidus of the rear-arc (solidus S2) is closer to the dry solidus than the one of the frontal arc (solidus S1). Therefore, the average degree of mantle melting of the rear-arc is

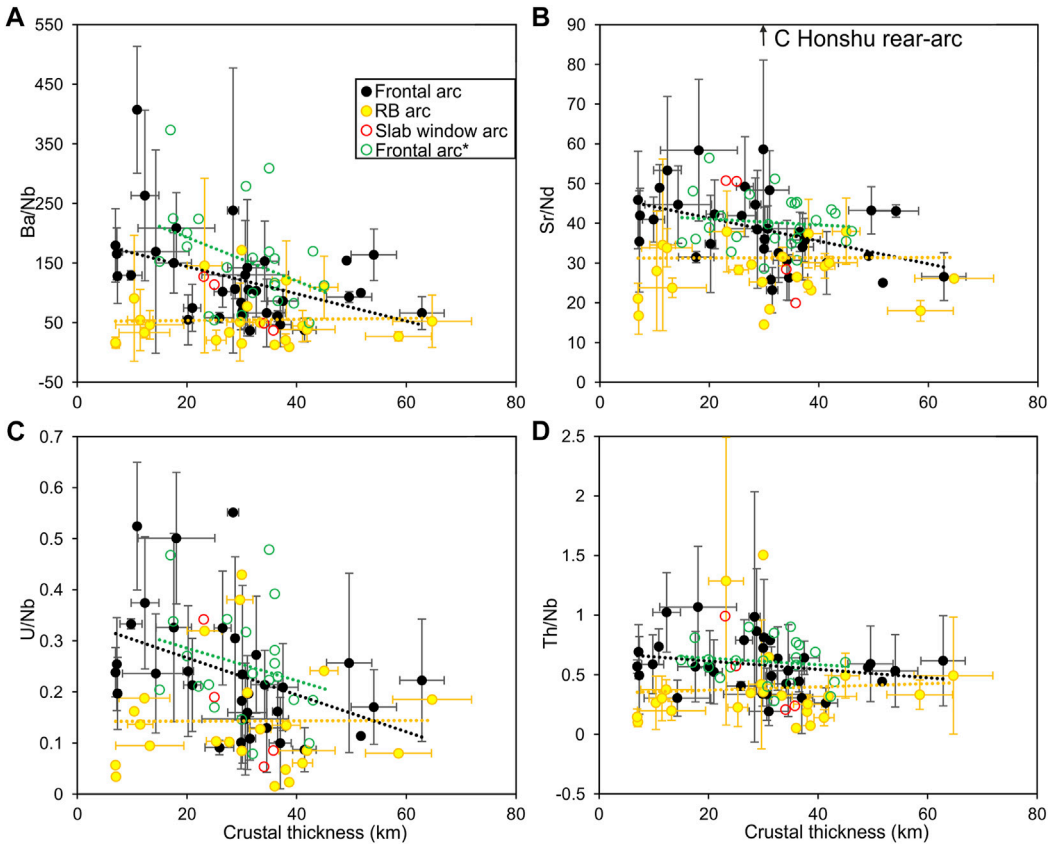

FIGURE 7
Comparison of trace element ratios between the frontal arc and rear-/back-arc sections. Crustal thickness vs. **(A)** Ba/Nb, **(B)** Sr/Nd and **(C)** U/Nb. Lower Ba/Nb, Sr/Nd, and U/Nb indicate the rear-/back-arc sections are less affected by aqueous fluids compared with the frontal arc sections. **(D)** Crustal thickness vs. Th/Nb. Lower Th/Nb indicates the rear-/back-arc sections are less affected by sediment melts.

smaller than that of the frontal arc giving rise to higher Zr/Yb or Nb/Yb in the rear-/back-arc (Figure 2).

In addition to the across-arc variation dictated by slab-derived aqueous fluids in terms of fluid mobile elements (represented by Ba/Nb, Sr/Nd, and U/Nb), whether along-arc variation affected by these aqueous fluids or not is also explored in this study. As can be seen from Figure 7, no significant correlation between crustal thickness and fluid mobile elements suggesting aqueous fluids in frontal arc magmas are not dictated by crustal thickness. Besides, Φ/100 vs. fluid mobile element indices in Figure 8A also shows no significant correlation. Furthermore, the components of Φ (i.e., slab age, convergent velocity, slab dip) along with sub-arc slab depth H show no significant correlation with fluid mobile elements of frontal arc rocks (and also rear-/back-arc rocks) (Figures 8B–E). All these indicate aqueous fluids in frontal arc magmas are not simply dictated by slab parameters and crustal thickness. The content of fluid mobile elements in frontal arc magmas could be affected by the initial slab hydration, slab dehydration and mantle metasomatism.

Firstly, oceanic lithosphere usually goes through alteration after its formation in middle ocean ridge prior to subducting. Alteration of oceanic crust differs in terms of the degree of alteration and the type of alteration. Hydrothermal alteration is intense in young and hot crust such as in middle ocean ridge and it weakens away from ridge as the crust ages and is covered by sediment (Staudigel, 2014). Different alteration types such as spilitization, epidotization and chloritization occurs due to the composition and age of oceanic crust and the type of the hydrothermal fluids (Hernández-Uribe et al., 2020). Fluids release in subduction zones are affected by alteration types and alteration degrees (Hernández-Uribe et al., 2020) and therefore oceanic lithosphere alteration imposes an effect on the content of fluid mobile elements in frontal arc rocks.

Secondly, slab dehydration in subduction zones is a complex process. Subducting slab is comprised of the uppermost sediment layer, the middle AOC layer, and the lowermost serpentinized peridotite layer with sediment dehydrating first and serpentinized peridotite the last (Rüpke et al., 2004). When the slab subducts to a shallow fore-arc level (<15 km; Bebout, 2013), the sediment and

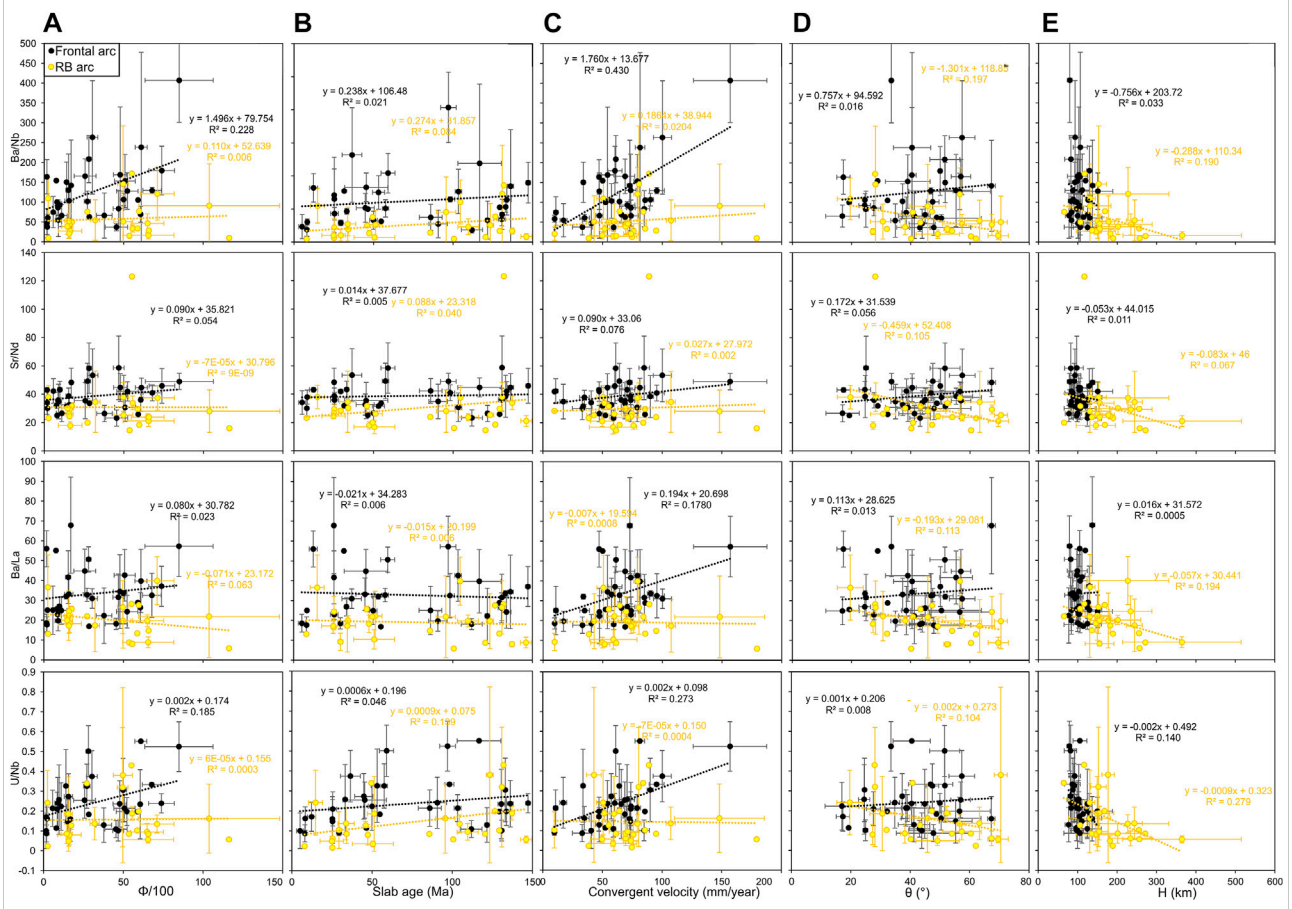

FIGURE 8
Slab thermal parameter **(A)**, slab age **(B)**, convergent velocity **(C)**, slab dip **(D)**, and slab depth **(E)** vs. elements mobile in aqueous fluids.

AOC layer experience large amounts of compaction, resulting in a mechanical expulsion of pore waters (Moore and Vrolijk, 1992). Beyond this depth of ~15 km, the AOC enters into the blueschist facies, in which the major hydrous minerals are chlorite, amphiboles, phengite, lawsonite (Sorensen, 1986). These hydrous minerals can dehydrate significantly to release large volume of aqueous fluids, through various continuous and discontinuous reaction beneath fore-arc or frontal arc or rear-/back-arc (Rüpke et al., 2004; van Keken et al., 2011; Schmidt and Poli, 2014). For example, the pressure-sensitive mineral amphibole breaks down at 2.2–2.4 GPa while small amount of water remaining in hydrous phases of AOC (e.g., lawsonite and phengite) might go further down to sub-arc depth (Schmidt and Poli, 2014; Niu and Green, 2018). However, recent studies show that aqueous fluids release completely before reaching ~60 km at hot subduction zones such as Cascadia while lawsonite can still survive to the sub-arc depth in cold subduction zone such as Honshu (Hernández-Uribe and Palin, 2019; Barber et al., 2022). Most of the fluid released from slab in the forearc depth will either serpentinize the cold corner of the mantle wedge, or eventually pass through to the ocean floor in the forearc region [e.g., Mariana arc, (Fryer et al., 1999; Fryer, 2012)]. Serpentine remains stable in hydrated slab mantle to at least 2 GPa regardless of slab thermal structure (Ulmer and Trommsdorff, 1995). It starts to dehydrate in slab sub-arc depth in hot subduction zones (Rüpke et al., 2004). Therefore, slab dehydration is controlled by continuous and discontinuous reactions of different hydrous minerals under different slab thermal condition. In addition, slab dehydration is also affected by slab geometry. Slab fractures facilitate hydrating slab mantle peridotite and the additional aqueous fluids released from this serpentinized mantle in fractured zones are evidenced in Aleutian arc (Singer et al., 2007; Manea et al., 2014) and Lesser Antilles (Cooper et al., 2020).

The relationship between slab thermal structure and slab parameters is unclear which further decorrelates slab parameters and aqueous fluids. Slab thermal parameter Φ is the first to represent slab thermal structure (Kirby et al., 1991). Some also use the product of convergent velocity and slab age as the indice (van Keken et al., 2011). More recently, Maunder et al. (2019) suggests slab temperature is controlled by slab age in slab-overriding plate decoupling depth (70–80 km). At slab sub-arc

depth, the slab mantle temperature is also negatively correlated with slab age but temperature of slab crust is dominated by convergent velocity. In addition to the slab parameters, slab thermal structure is also affected by the thickness of the overriding plate with slab AOC cooling down due to increasing thickness of upper plate (Holt and Condit, 2021). Besides, slab thermal structure is dynamic and it changes as subduction zone evolve from subduction initiation to mature subduction (Holt and Condit, 2021). The mantle wedge for arcs at different stage goes through metasomatism by fluids derived from different slab dehydration.

Thirdly, the processes of mantle wedge metasomatism are also unclear. The first model is that large volume of aqueous fluids release in the fore-arc and metasomatize the fore-arc mantle wedge as indicated by the serpentinite seamount in IBM (Fryer et al., 1999; Fryer, 2012). These hydrous minerals (e.g., serpentine) can be transported downward by movement of subducting slab and releases their fluids to trigger flux melting (Hattori and Guillot, 2003). The fluid release of the hydrous mantle wedge might be a complex process as suggested by geodynamic modelling (Davies and Stevenson, 1992). This is supported by geochemical evidence as boron isotope of the arc rocks is too heavy and need materials from the serpentinized fore-arc (Tonarini et al., 2011; Leeman et al., 2017). The second model is melange-style melting (Marschall and Schumacher, 2012; Nielsen and Marschall, 2017). Bulk sediment and AOC mix with serpentinized mantle wedge peridotite to form a buoyant melange in the fore-arc mantle wedge. This melange goes up and away from trench to the hot corner under frontal arc where it partially melts to form arc magmas. Similar to the first model, it is beneath fore-arc rather than frontal arc where aqueous fluids release from AOC. The conventional model of mantle wedge melting is AOC fluids along with sediment melts release from slab beneath frontal arc (Ryan and Chauvel, 2014; Schmidt and Poli, 2014). The serpentinized peridotite can also release aqueous fluids beneath frontal arc which either mix with the AOC fluids or facilitate melting of AOC and sediment (Ulmer and Trommsdorff, 1995; Rüpke et al., 2004). This mixture of aqueous fluids and melts from different layers of the subducting slab percolates upward through mantle wedge to trigger mantle melting where frontal arc magmas derive. Therefore, this model differ with first two models in that slab dehydration occurs under frontal arc rather than fore-arc. Besides, sediment melt rather than bulk sediment is suggested to play a role in arc magmatism. All these complex processes make aqueous fluids in arc magmas hard to constrain.

Subduction zone magmatism is caused by a series of complex processes affected by the subducting plate and overriding plate. The aqueous fluids are controlled by oceanic alteration prior to subducting, slab dehydration, and mantle metasomatism with the exact processes highly debated. Even though the mechanism of mantle wedge melting is unclear, the melting degrees are modulated by the thickness of the overriding plate as revealed by the elements immobile in aqueous fluids. Besides, mass transfer even for fluid immobile elements are common especially in subduction zones with hot slab thermal structure.

4 Conclusion

The thickness of the overriding plate exerts its effect on the composition of primitive arc magmas through mantle melting degrees. The mantle wedge geotherm is deepened or the melting column shortens under thick crust/lithosphere so the degrees of mantle melting decrease. Trace element ratio Zr/Yb and Nb/Yb in frontal arc rocks show a good positive correlation with crustal thickness which are also found in rear-/back-arcs. Crustal thickness gives rise to along-arc variations for both systems.

The slab thermal structure influences the composition of arc basalts (e.g., elements immobile in aqueous fluids) by mass transfer from the subducting slab to the mantle wedge. It contributes to the across- and along-arc variations in incompatible elements (e.g., Zr/Yb and Nb/Yb) as well as in isotopic characteristics (i.e., $^{143}Nd/^{144}Nd$). Hot subduction zones with a low value of slab thermal parameter can liberate AOC melts apart from sediment components.

Slab-derived aqueous fluids play an important role in across-arc variations through mass transfer. The subducting slab releases less aqueous fluids in the rear-/back-arc than the frontal arc resulting in depletion of aqueous fluids elements in rear-/back-arcs. Besides, less aqueous fluids give rise to smaller degrees of mantle melting and therefore higher Zr/Yb and Nb/Yb values in the rear-/back-arc rocks. No significant correlations between aqueous fluids and slab parameters indicate the volume of aqueous fluids in arc magmas are controlled by complex processes. Oceanic lithosphere alteration prior to subducting, slab dehydration, slab geometry, and factors unrelated to slab such as the mechanism of mantle wedge metasomatism and melting and thickness of overriding plate possibly impose effects on aqueous fluids in primitive arc magmas.

Author contributions

JW: Investigation, methodology, conceptualization, writing original draft, review and editing. MG: Conceptualization, writing, reviewing and editing. WS: Reviewing and editing. LM: Reviewing and editing. ZL: Reviewing and editing. GS: Reviewing and editing. LC: Reviewing.

Funding

This work is supported by China Scholarship Council (grant #201606400067) and Cardiff University which provide the financial support for the first author's PhD.

Acknowledgments

The first author thanks China Scholarship Council (grant #201606400067) and Cardiff University for the PhD support as this work is mainly done during the first author's PhD study. Thanks go to Prof. Huw Davies who enlightens the first author on some key questions in this paper. Thanks go to David Buchs, Prof. Yongfei Zheng, and Lilong Yan as this paper benefits a lot from the scientific discussions with them.

Conflict of interest

The authors declare that the research was conducted in the absence of any commercial or financial relationships that could be construed as a potential conflict of interest.

Publisher's note

Supplementary material

The Supplementary Material for this article can be found online at: https://www.frontiersin.org/articles/10.3389/feart.2022.1055255/full#supplementary-material

References

Abratis, M., Wörner, G., Worner, G., Wörner, G., Worner, G., and Wörner, G. (2001). Ridge collision, slab-window formation, and the flux of Pacific asthenosphere into the Caribbean realm. *Geology* 29, 127–130. doi:10.1130/0091-7613(2001)029<0127:rcswfa>2.0.co;2

Ancellin, M.-A., Samaniego, P., Vlastélic, I., Nauret, F., Gannoun, A., and Hidalgo, S. (2017). Across-arc versus along-arc Sr-Nd-Pb isotope variations in the Ecuadorian volcanic arc. *Geochem. Geophys. Geosystems* 18, 1163–1188. doi:10.1002/2016GC006679

Asimow, P. D., and Langmuir, C. H. (2003). The importance of water to oceanic mantle melting regimes. *Nature* 421, 815–820. doi:10.1038/nature01429

Barber, N. D., Edmonds, M., Jenner, F., and Williams, H. (2022). Global Ba/Nb systematics in arc magmas reflect the depths of mineral dehydration in subducted slabs. *Geology* 50, 1438–1442. doi:10.1130/g50447.1

Barber, N. D., Edmonds, M., Jenner, F., Audétat, A., and Williams, H. (2021). Amphibole control on copper systematics in arcs: Insights from the analysis of global datasets. *Geochim. Cosmochim. Acta* 307, 192–211. doi:10.1016/j.gca.2021.05.034

Bebout, G. (2013). *Chemical and isotopic cycling in subduction zones*. 2nd ed. Amsterdam, Netherlands: Elsevier. doi:10.1016/B978-0-08-095975-7.01401-7

Beier, C., Turner, S. P., Haase, K. M., Pearce, J. A., Münker, C., and Regelous, M. (2017). Trace element and isotope geochemistry of the northern and central Tongan islands with an emphasis on the Genesis of high Nb/Ta signatures at the northern volcanoes of tafahi and niuatoputapu. *J. Petrology* 58, 1073–1106. doi:10.1093/petrology/egx047

Bird, P. (2003). An updated digital model of plate boundaries. *Geochem. Geophys. Geosystems* 4. doi:10.1029/2001GC000252

Brenan, J. M., Shaw, H. F., Ryerson, F. J., and Phinney, D. L. (1995). Mineral-aqueous fluid partitioning of trace elements at 900°C and 2.0 GPa: Constraints on the trace element chemistry of mantle and deep crustal fluids. *Geochim. Cosmochim. Acta* 59, 3331–3350. doi:10.1016/0016-7037(95)00215-L

Chen, C., Lee, C. T. A., Tang, M., Biddle, K., and Sun, W. (2020). Lithium systematics in global arc magmas and the importance of crustal thickening for lithium enrichment. *Nat. Commun.* 11, 5313–5318. doi:10.1038/s41467-020-19106-z

Chiaradia, M. (2015). Crustal thickness control on Sr/Y signatures of recent arc magmas: An earth scale perspective. *Sci. Rep.* 5, 8115. doi:10.1038/srep08115

Cooper, G. F., Macpherson, C. G., Blundy, J. D., Maunder, B., Allen, R. W., Goes, S., et al. (2020). Variable water input controls evolution of the Lesser Antilles volcanic arc. *Nature* 582, 525–529. doi:10.1038/s41586-020-2407-5

Cousens, B. L., Henry, C. D., Harvey, B. J., Brownrigg, T., Prytulak, J., and Allan, J. F. (2011). Secular variations in magmatism during a continental arc to post-arc transition: Plio-Pleistocene volcanism in the Lake Tahoe/Truckee area, Northern Sierra Nevada, California. *Lithos* 123, 225–242. doi:10.1016/j.lithos.2010.09.009

Curie, C. A., and Hyndman, R. D. (2006). The thermal structure of subduction zone back arcs. *J. Geophys Res. Solid Earth* 111, B08404–B08422. doi:10.1029/2005JB004024

Currie, C. A., Wang, K., Hyndman, R. D., and He, J. (2004). The thermal effects of steady-state slab-driven mantle flow above a subducting plate: The Cascadia subduction zone and backarc. *Earth Planet Sci. Lett.* 223, 35–48. doi:10.1016/j.epsl.2004.04.020

Davies, J. H., and Stevenson, D. J. (1992). Physical model of source region of subduction zone volcanics. *J. Geophys. Res.* 97, 2037–2070. doi:10.1029/91jb02571

Davies, J. H. (1999). The role of hydraulic fractures and intermediate-depth earthquakes in generating subduction-zone magmatism. *Nature* 398, 142–145. doi:10.1038/18202

Defant, M. J., and Drummond, M. S. (1990). Derivation of some modern arc magmas by melting of young subducted lithosphere. *Nature* 347, 662–665. doi:10.1038/347662a0

Duggen, S., Portnyagin, M., Baker, J., Ulfbeck, D., Hoernle, K., Garbe-Schönberg, D., et al. (2007). Drastic shift in lava geochemistry in the volcanic-front to rear-arc region of the Southern Kamchatkan subduction zone: Evidence for the transition from slab surface dehydration to sediment melting. *Geochim. Cosmochim. Acta* 71, 452–480. doi:10.1016/j.gca.2006.09.018

Edwards, C., Menzies, M., and Thirlwall, M. (1991). Evidence from muriah, Indonesia, for the interplay of supra-subduction zone and intraplate processes in the Genesis of potassic alkaline magmas. *J. Petrology* 32, 555–592. doi:10.1093/petrology/32.3.555

Edwards, C. M. H., Menzies, M. A., Thirlwall, M. F., Morris, J. D., Leeman, W. P., and Harmon, R. S. (1994). The transition to potassic alkaline volcanism in island arcs: The ringgit - beser complex, east java, Indonesia. *J. Petrology* 35, 1557–1595. doi:10.1093/petrology/35.6.1557

Elliott, T., Plank, T., Zindler, A., White, W., and Bourdon, B. (1997). Element transport from slab to volcanic front at the Mariana arc. *J. Geophys Res.* 102 (14), 14991–15019. doi:10.1029/97jb00788

Elliott, T. (2003). "Tracers of the slab," in *Inside the subduction factory* (Washington, DC, USA: AGU), 23–45. doi:10.1029/138GM03

Farner, M. J., and Lee, C. T. A. (2017). Effects of crustal thickness on magmatic differentiation in subduction zone volcanism: A global study. *Earth Planet Sci. Lett.* 470, 96–107. doi:10.1016/j.epsl.2017.04.025

Fryer, P. (2012). Serpentinite mud volcanism: Observations, processes, and implications. *Ann. Rev. Mar. Sci.* 4, 345–373. doi:10.1146/annurev-marine-120710-100922

Fryer, P., Wheat, C. G., and Mottl, M. J. (1999). Mariana blueschist mud volcanism: Implications for conditions within the subduction zone. *Geology* 27, 103–106. doi:10.1130/0091-7613(1999)027<0103:mbmvif>2.3.co;2

Gaetani, G. A., and Grove, T. L. (2004). Experimental constraints on melt generation in the mantle wedge. *Inside Subduction Fact.*, 107–134. doi:10.1029/138GM07

Global Volcanism Program (2013). *Volcanoes of the World*, v. 4.10.1 (29 Jun 2021). Editor E. Venzke (Smithsonian Institution). Downloaded (Aug 21, 2021)

Goldstein, S. L., O'Nions, R. K., and Hamilton, P. J. (1984). A SmNd isotopic study of atmospheric dusts and particulates from major river systems. *Earth Planet Sci. Lett.* 70, 221–236. doi:10.1016/0012-821X(84)90007-4

Green, D. H., Hibberson, W. O., Kovács, I., and Rosenthal, A. (2010). Water and its influence on the lithosphere-asthenosphere boundary. *Nature* 467, 448–451. doi:10.1038/nature09369

Grove, T. L., Chatterjee, N., Parman, S. W., and Médard, E. (2006). The influence of H2O on mantle wedge melting. *Earth Planet Sci. Lett.* 249, 74–89. doi:10.1016/j.epsl.2006.06.043

Grove, T. L., Till, C. B., and Krawczynski, M. J. (2012). The role of H 2O in subduction zone magmatism. *Annu. Rev. Earth Planet Sci.* 40, 413–439. doi:10.1146/annurev-earth-042711-105310

Grove, T. L., Till, C. B., Lev, E., Chatterjee, N., and Médard, E. (2009). Kinematic variables and water transport control the formation and location of arc volcanoes. *Nature* 459, 694–697. doi:10.1038/nature08044

Gutiérrez, F., Gioncada, A., González Ferran, O., Lahsen, A., and Mazzuoli, R. (2005). The Hudson Volcano and surrounding monogenetic centres (Chilean Patagonia): An example of volcanism associated with ridge-Trench collision environment. *J. Volcanol. Geotherm. Res.* 145, 207–233. doi:10.1016/j.jvolgeores.2005.01.014

Hall, P. S. (2012). On the thermal evolution of the mantle wedge at subduction zones. *Phys. Earth Planet. Interiors* 198-199, 9–27. doi:10.1016/j.pepi.2012.03.004

Hattori, K. H., and Guillot, S. (2003). Volcanic fronts form as a consequence of serpentinite dehydration in the forearc mantle wedge. *Geology* 31, 525–528. doi:10.1130/0091-7613(2003)031<0525:vffaac>2.0.co;2

Hauff, F., Hoernle, K., and Schmidt, A. (2003). Sr-Nd-Pb composition of Mesozoic Pacific oceanic crust (Site 1149 and 801, ODP Leg 185): Implications for alteration of ocean crust and the input into the Izu-Bonin-Mariana subduction system. *Geochem. Geophys. Geosystems* 4. doi:10.1029/2002GC000421

Hawkesworth, C. J., Gallagher, K., Hergt, J. M., and McDermott, F. (1993). Mantle and slab contributions in arc magmas. *Annu. Rev. Earth Planet Sci.* 21, 175–204. doi:10.1146/annurev.ea.21.050193.001135

Hayes, G. P., Moore, G. L., Portner, D. E., Hearne, M., Flamme, H., Furtney, M., et al. (2018). Slab2, a comprehensive subduction zone geometry model. *Science* 362, 58–61. doi:10.1126/science.aat4723

Hermann, J., and Rubatto, D. (2009). Accessory phase control on the trace element signature of sediment melts in subduction zones. *Chem. Geol.* 265, 512–526. doi:10.1016/j.chemgeo.2009.05.018

Hernández-Uribe, D., Palin, R. M., Cone, K. A., and Cao, W. (2020). Petrological implications of seafloor hydrothermal alteration of subducted mid-ocean ridge basalt. *J. Petrology* 61, egaa086. doi:10.1093/petrology/egaa086

Hernández-Uribe, D., and Palin, R. M. (2019). A revised petrological model for subducted oceanic crust: Insights from phase equilibrium modelling. *J. Metamorph. Geol.* 37, 745–768. doi:10.1111/jmg.12483

Holt, A. F., and Condit, C. B. (2021). Slab temperature evolution over the lifetime of a subduction zone. *Geochem. Geophys. Geosystems* 22, e2020GC009476. doi:10.1029/2020gc009476

Ishikawa, T., and Nakamura, E. (1994). Origin of the slab component in arc lavas from across-arc variation of B and Pb isotopes. *Nature* 370, 205–208. doi:10.1038/370205a0

Johnston, F. K. B., Turchyn, A. V., and Edmonds, M. (2011). Decarbonation efficiency in subduction zones: Implications for warm Cretaceous climates. *Earth Planet Sci. Lett.* 303, 143–152. doi:10.1016/j.epsl.2010.12.049

Katz, R. F., Spiegelman, M., and Langmuir, C. H. (2003). A new parameterization of hydrous mantle melting. *Geochem. Geophys. Geosystems* 4. doi:10.1029/2002GC000433

Kelemen, P. B., Hanghoj, K., and Greene, A. R. (2013). *One view of the geochemistry of subduction-related magmatic arcs, with an emphasis on primitive andesite and lower crust*. 4th ed. Amsterdam, Netherlands: Elsevier. doi:10.1016/B978-0-08-095975-7.00516-7

Kessel, R., Schmidt, M. W., Ulmer, P., and Pettke, T. (2005). Trace element signature of subduction-zone fluids, melts and supercritical liquids at 120-180 km depth. *Nature* 437, 724–727. doi:10.1038/nature03971

Kirby, S. H., Durham, W. B., and Stern, L. A. (1991). Mantle phase changes and deep-earthquake faulting in subducting lithosphere. *Science* 252, 216–225. doi:10.1126/science.252.5003.216

Klein, E. M., and Langmuir, C. H. (1987). Global correlations of ocean ridge basalt chemistry with axial depth and crustal thickness. *J. Geophys. Res.* 92, 8089–8115. doi:10.1029/jb092ib08p08089

Langmuir, C. H., Klein, E. M., and Plank, T. (1992). "Petrological systematics of mid-ocean ridge basalts: Constraints on melt generation beneath ocean ridges," in *Mantle flow and melt generation at mid-ocean ridges* (Washington, DC, USA: AGU), 183–280. doi:10.1029/GM071p0183

Laske, G., Masters, G., Ma, Z., and Pasyanos, M. (2013). Update on CRUST1.0 - a 1-degree global model of Earth's crust. *Abstr. EGU2013-2658 Present. A. T. 2013 Geophys. Res. Abstr.* 15, 2658.

Lee, C. T. A., Luffi, P., Chin, E. J., Bouchet, R., Dasgupta, R., Morton, D. M., et al. (2012). Copper systematics in arc magmas and implications for crust-mantle differentiation. *Science* 335, 64–68. doi:10.1126/science.1217313

Lee, C. T. A., Luffi, P., Plank, T., Dalton, H., and Leeman, W. P. (2009). Constraints on the depths and temperatures of basaltic magma generation on Earth and other terrestrial planets using new thermobarometers for mafic magmas. *Earth Planet Sci. Lett.* 279, 20–33. doi:10.1016/j.epsl.2008.12.020

Lee, C. T. A., Morton, D. M., Kistler, R. W., and Baird, A. K. (2007). Petrology and tectonics of Phanerozoic continent formation: From island arcs to accretion and continental arc magmatism. *Earth Planet Sci. Lett.* 263, 370–387. doi:10.1016/j.epsl.2007.09.025

Leeman, W. P., Carr, M. J., and Morris, J. D. (1994). Boron geochemistry of the central American volcanic arc: Constraints on the Genesis of subduction-related magmas. *Geochim. Cosmochim. Acta* 58, 149–168. doi:10.1016/0016-7037(94)90453-7

Leeman, W. P., Tonarini, S., and Turner, S. (2017). Boron isotope variations in T onga-K ermadec-N ew Z ealand arc lavas: Implications for the origin of subduction components and mantle influences. *Geochem. Geophys. Geosystems* 18, 1126–1162. doi:10.1002/2016gc006523

Manea, V. C., Leeman, W. P., Gerya, T., Manea, M., and Zhu, G. (2014). Subduction of fracture zones controls mantle melting and geochemical signature above slabs. *Nat. Commun.* 5, 5095–5110. doi:10.1038/ncomms6095

Mantle, G. W., and Collins, W. J. (2008). Quantifying crustal thickness variations in evolving orogens: Correlation between arc basalt composition and Moho depth. *Geology* 36, 87–90. doi:10.1130/g24095a.1

Marschall, H. R., and Schumacher, J. C. (2012). Arc magmas sourced from mélange diapirs in subduction zones. *Nat. Geosci.* 5, 862–867.

Maunder, B., van Hunen, J., Bouilhol, P., and Magni, V. (2019). Modeling slab temperature: A reevaluation of the thermal parameter. *Geochem. Geophys. Geosystems* 20, 673–687. doi:10.1029/2018GC007641

Moore, J. C., and Vrolijk, P. (1992). Fluids in accretionary prisms. *Rev. Geophys.* 30, 113–135. doi:10.1029/92rg00201

Müller, R. D., Sdrolias, M., Gaina, C., and Roest, W. R. (2008). Age, spreading rates, and spreading asymmetry of the world's ocean crust. *Geochem. Geophys. Geosystems* 9, 1–19. doi:10.1029/2007GC001743

Nielsen, S. G., and Marschall, H. R. (2017). Geochemical evidence for mélange melting in global arcs. *Sci. Adv.* 3, e1602402. doi:10.1126/sciadv.1602402

Niu, Y., and Green, D. H. (2018). The petrological control on the lithosphere-asthenosphere boundary (LAB) beneath ocean basins. *Earth Sci. Rev.* 185, 301–307. doi:10.1016/j.earscirev.2018.06.011

Niu, Y. (2021). Lithosphere thickness controls the extent of mantle melting, depth of melt extraction and basalt compositions in all tectonic settings on Earth – a review and new perspectives. *Earth Sci. Rev.* 217, 103614. doi:10.1016/j.earscirev.2021.103614

Niu, Y. (1997). Mantle melting and melt extraction processes beneath ocean ridges: Evidence from abyssal peridotites. *J. Petrology* 38, 1047–1074. doi:10.1093/petroj/38.8.1047

Patino, L. C., Carr, M. J., and Feigenson, M. D. (2000). Local and regional variations in Central American arc lavas controlled by variations in subducted sediment input. *Contrib. Mineral. Pet.* 138, 265–283. Available at:. doi:10.1007/s004100050562

Pearce, J. A., Stern, R. J., Bloomer, S. H., and Fryer, P. (2005). Geochemical mapping of the Mariana arc-basin system: Implications for the nature and distribution of subduction components. *Geochem. Geophys. Geosystems* 6. doi:10.1029/2004GC000895

Pearce, J. A., and Parkinson, I. J. (1993). Trace element models for mantle melting: Application to volcanic arc petrogenesis. *Geol. Soc. Lond. Spec. Publ.* 76, 373–403. doi:10.1144/gsl.sp.1993.076.01.19

Pearce, J. A., and Peate, D. W. (1995). Tectonic implications of the composition of volcanic arc magmas. *Annu. Rev. Earth Planet Sci.* 23, 251–285. doi:10.1146/annurev.ea.23.050195.001343

Peate, D. W., Pearce, J. A., Hawkesworth, C. J., Colley, H., Edwards, C. M. H., and Hirose, K. (1997). Geochemical variations in Vanuatu arc lavas: The role of subducted material and a variable mantle wedge composition. *J. Petrology* 38, 1331–1358. doi:10.1093/petroj/38.10.1331

Perrin, A., Goes, S., Prytulak, J., Rondenay, S., and Davies, D. R. (2018). Mantle wedge temperatures and their potential relation to volcanic arc location. *Earth Planet Sci. Lett.* 501, 67–77. doi:10.1016/j.epsl.2018.08.011

Plank, T., and Langmuir, C. H. (1993). Tracing trace elements from sediment input to volcanic output at subduction zones. *Nature* 362, 739–743. doi:10.1038/362739a0

Plank, T. (2005). Constraints from Thorium/Lanthanum on sediment recycling at subduction zones and the evolution of the continents. *J. Petrology* 46, 921–944. doi:10.1093/petrology/egi005

Plank, T., and Langmuir, C. H. (1988). An evaluation of the global variations in the major element chemistry of arc basalts. *Earth Planet Sci. Lett.* 90, 349–370. doi:10.1016/0012-821x(88)90135-5

Plank, T. (2013). *The chemical composition of subducting sediments*. 2nd ed. Amsterdam, Netherlands,: Elsevier. doi:10.1016/B978-0-08-095975-7.00319-3

Rüpke, L. H., Morgan, J. P., Hort, M., and Connolly, J. A. D. (2004). Serpentine and the subduction zone water cycle. *Earth Planet Sci. Lett.* 223, 17–34. doi:10.1016/j.epsl.2004.04.018

Ryan, H. F., and Marlow, M. S. (1988). Multichannel seismic-reflection data collected at the intersection of the Mussau and Manus trenches, Papua New Guinea. U.S. Geological Survey. https://archives.datapages.com/data/meta/circ_pac/0010/0203_f_firstpage.pdf.

Ryan, J. G., and Chauvel, C. (2014). *The subduction-zone filter and the impact of recycled materials on the evolution of the mantle*. Amsterdam, Netherlands: sciencedirect. doi:10.1016/B978-0-08-095975-7.00211-4

Ryan, J. G., Morris, J., Tera, F., Leeman, W. P., and Tsvetkov, A. (1995). Cross-arc geochemical variations in the Kurile arc as a function of slab depth. *Science* 270, 625–627. doi:10.1126/science.270.5236.625

Singer, B. S., Jicha, B. R., Leeman, W. P., Rogers, N. W., Thirlwall, M. F., Ryan, J., et al. (2007). Along-strike trace element and isotopic variation in Aleutian Island arc basalt: Subduction melts sediments and dehydrates serpentine. *J. Geophys Res. Solid Earth* 112, B06206. doi:10.1029/2006jb004897

Schmidt, M. W., and Jagoutz, O. (2017). The global systematics of primitive arc melts. *Geochem. Geophys. Geosystems* 18, 2817–2854. doi:10.1002/2016GC006699

Schmidt, M. W., and Poli, S. (2014). Editors H. D. Holland and Turekian, K. K. 2nd Ed. (Amsterdam, Netherlands: Elsevier), 669–701. doi:10.1016/B978-0-08-095975-7.00321-1*Devolatilization during subduction*

Schmidt, M. W., and Poli, S. (1998). Experimentally based water budgets for dehydrating slabs and consequences for arc magma generation. *Earth Planet Sci. Lett.* 163, 361–379. doi:10.1016/S0012-821X(98)00142-3

Schuth, S., Münker, C., König, S., Qopoto, C., Basi, S., Garbe-Schönberg, D., et al. (2009). Petrogenesis of lavas along the Solomon Island Arc, SW Pacific: Coupling of compositional variations and subduction zone geometry. *J. Petrology* 50, 781–811. doi:10.1093/petrology/egp019

Shu, Y., Nielsen, S. G., Zeng, Z., Shinjo, R., Blusztajn, J., Wang, X., et al. (2017). Tracing subducted sediment inputs to the Ryukyu arc-Okinawa Trough system: Evidence from thallium isotopes. *Geochim. Cosmochim. Acta* 217, 462–491. doi:10.1016/j.gca.2017.08.035

Skora, S., and Blundy, J. (2010). High-pressure hydrous phase relations of radiolarian clay and implications for the involvement of subducted sediment in arc magmatism. *J. Petrology* 51, 2211–2243. doi:10.1093/petrology/egq054

Sorensen, S. S. (1986). *Petrologic and geochemical comparison of the blueschist and greenschist units of the Catalina Schist terrane, southern California*, 164. Boulder, CO, USA.: Geological Society of America Memoir, 59–75. doi:10.1130/MEM164-p59

Staudigel, H. (2014). *Chemical fluxes from hydrothermal alteration of the oceanic crust*. Amsterdam, Netherlands: Elsevier, 583–606. doi:10.1016/B978-0-08-095975-7.00318-1

Syracuse, E. M., and Abers, G. A. (2006). Global compilation of variations in slab depth beneath arc volcanoes and implications. *Geochem. Geophys. Geosystems* 7. doi:10.1029/2005GC001045

Tatsumi, Y., Hamilton, D. L., and Nesbitt, R. W. (1986). Chemical characteristics of fluid phase released from a subducted lithosphere and origin of arc magmas: Evidence from high-pressure experiments and natural rocks. *J. Volcanol. Geotherm. Res.* 29, 293–309. doi:10.1016/0377-0273(86)90049-1

Tatsumi, Y. (2005). The subduction factory: How it operates in the evolving earth. *GSA today* 15, 4. doi:10.1130/1052-5173(2005)015[4:tsfhio]2.0.co;2

Taylor, R. N., and Nesbitt, R. W. (1998). Isotopic characteristics of subduction fluids in an intra-oceanic setting, Izu-Bonin Arc, Japan. *Earth Planet Sci. Lett.* 164, 79–98. doi:10.1016/S0012-821X(98)00182-4

Thorkelson, D. J., and Breitsprecher, K. (2005). Partial melting of slab window margins: Genesis of adakitic and non-adakitic magmas. *Lithos* 79, 25–41. doi:10.1016/j.lithos.2004.04.049

Thorkelson, D. J. (1996). Subduction of diverging plates and the principles of slab window formation. *Tectonophysics* 255, 47–63. doi:10.1016/0040-1951(95)00106-9

Tollstrup, D., Gill, J., Kent, A., Prinkey, D., Williams, R., Tamura, Y., et al. (2010). Across-arc geochemical trends in the Izu-Bonin arc: Contributions from the subducting slab, revisited. *Geochem. Geophys. Geosystems* 11. doi:10.1029/2009GC002847

Tonarini, S., Leeman, W. P., and Leat, P. T. (2011). Subduction erosion of forearc mantle wedge implicated in the Genesis of the South sandwich island (SSI) arc: Evidence from boron isotope systematics. *Earth Planet Sci. Lett.* 301, 275–284. doi:10.1016/j.epsl.2010.11.008

Tregoning, P., and Gorbatov, A. (2004). Evidence for active subduction at the new Guinea trench. *Geophys Res. Lett.* 31. doi:10.1029/2004gl020190

Turner, S. J., Langmuir, C. H., Katz, R. F., Dungan, M. A., and Escrig, S. (2016). Parental arc magma compositions dominantly controlled by mantle-wedge thermal structure. *Nat. Geosci.* 9, 772–776. doi:10.1038/ngeo2788

Turner, S. J., and Langmuir, C. H. (2015). What processes control the chemical compositions of arc front stratovolcanoes? *Geochem. Geophys. Geosystems* 16, 1865–1893. doi:10.1002/2014gc005633

Ulmer, P., and Trommsdorff, V. (1995). Serpentine stability to mantle depths and subduction-related magmatism. *Science* 268, 858–861. doi:10.1126/science.268.5212.858

van Keken, P. E., Hacker, B. R., Syracuse, E. M., and Abers, G. A. (2011). Subduction factory: 4. Depth-dependent flux of H2O from subducting slabs worldwide. *J. Geophys Res. Solid Earth* 116, B01401. doi:10.1029/2010jb007922

Verma, S. P., Torres-Sánchez, D., Velasco-Tapia, F., Subramanyam, K. S. V., Manikyamba, C., and Bhutani, R. (2016). Geochemistry and petrogenesis of extension-related magmas close to the volcanic front of the central part of the Trans-Mexican Volcanic Belt. *J. South Am. Earth Sci.* 72, 126–136. doi:10.1016/j.jsames.2016.08.006

Wendt, J. I., Regelous, M., Collerson, K. T., and Ewart, A. (1997). Evidence for a contribution from two mantle plumes to island-arc lavas from northern Tonga. *Geology* 25 (7), 611–614.

Werner, R., Hoernle, K., Barckhausen, U., and Hauff, F. (2003). Geodynamic evolution of the Galápagos hot spot system (Central East Pacific) over the past 20 m.y.: Constraints from morphology, geochemistry, and magnetic anomalies. *Geochem. Geophys. Geosystems* 4, 1108. doi:10.1029/2003GC000576

White, W. M., and Klein, E. M. (2013). *Composition of the oceanic crust*. 2nd ed. Amsterdam, Netherlands: Elsevier. doi:10.1016/B978-0-08-095975-7.00315-6

Woodhead, J. D., Eggins, S. M., and Johnson, R. W. (1998). Magma Genesis in the new britain island arc: Further insights into melting and mass transfer processes. *J. Petrology* 39, 1641–1668. doi:10.1093/petroj/39.9.1641

Woodhead, J., Eggins, S., and Gamble, J. (1993). High field strength and transition element systematics in island arc and back-arc basin basalts: Evidence for multi-phase melt extraction and a depleted mantle wedge. *Earth Planet Sci. Lett.* 114, 491–504. doi:10.1016/0012-821X(93)90078-N

Zellmer, G. F. (2008). Some first-order observations on magma transfer from mantle wedge to upper crust at volcanic arcs. *Geol. Soc. Spec. Publ.* 304, 15–31. doi:10.1144/SP304.2

Zheng, Y. F. (2019). Subduction zone geochemistry. *Geosci. Front.* 10, 1223–1254. doi:10.1016/j.gsf.2019.02.003

Zheng, Y. F., Xu, Z., Chen, L., Dai, L. Q., and Zhao, Z. F. (2020). Chemical geodynamics of mafic magmatism above subduction zones. *J. Asian Earth Sci.* 194, 104185. doi:10.1016/j.jseaes.2019.104185